

## Is there elliptic flow without transverse flow?

P. Huovinen<sup>a\*</sup>, P.F. Kolb<sup>b,c</sup> and U. Heinz<sup>c</sup>

<sup>a</sup>Lawrence Berkeley National Laboratory, Berkeley, USA

<sup>b</sup>Institut für Theoretische Physik, Universität Regensburg, Regensburg, Germany

<sup>c</sup>Department of Physics, The Ohio State University, Columbus, USA

Azimuthal anisotropy of final particle distributions was originally introduced as a signature of transverse collective flow [1]. We show that finite anisotropy in momentum space can result solely from the shape of the particle emitting source. However, by comparing the differential anisotropy to recent data from STAR collaboration [2,3] we can exclude such a scenario, but instead show that the data favour strong flow as resulting from a hydrodynamical evolution [4,5].

### 1. Bjorken Brick

The intensity of particles emitted from a steady thermal source depends on the size of the source facing the direction of emitted particles. If the shape of such a source is not azimuthally symmetric, the particle yield is anisotropic too. Thus it is easy to parametrize a source with an essentially arbitrary value of the elliptic flow coefficient  $v_2$ , but the transverse momentum dependence of the differential  $v_2(p_t)$  is much less trivial.

To gain insight what kind of elliptic flow might result from surface effects only, we constructed a simple parametrization of the source. Let us assume that the longitudinal expansion of the source is boost invariant, but that the source does not expand transversally at all. To simplify the calculation we take the source to be rectangular in transverse plane and to have a constant temperature  $T$ . Particle emission now takes place on the surfaces of the system during its lifetime (from thermalization time  $\tau_0$  until time  $t$ ) and from its entire volume at final breakup at time  $t$  (see Figs. 1 and 2). Unlike in [6], where the source was parametrized using a Gaussian profile, our source contains emission also through surfaces which normal vectors are spacelike. If these surfaces are opaque, this allows us to obtain finite  $v_2$  even if transverse flow is absent.

We calculate particle distributions using a modified Cooper-Frye procedure [7]:

$$E \frac{dN}{d^3p} = \int d\sigma_\mu p^\mu f(p \cdot u, T) \Theta(d\sigma_\mu p^\mu), \quad (1)$$

where the  $\Theta$ -function is needed to remove negative contributions to particle number. For the freeze-out surface described above, the integral can be calculated analytically. Using

---

\*P.H. acknowledges financial support from the DOE under Contract No. DE-AC03-76SF00098.

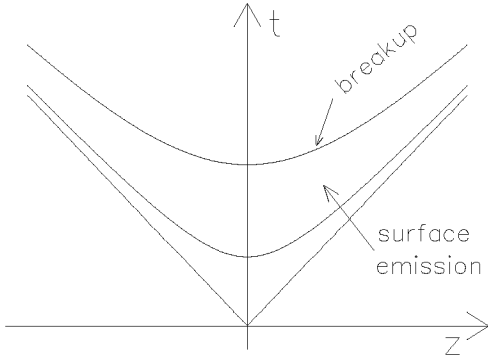


Figure 1. Boost-invariant expansion of the source and emission in two stages.

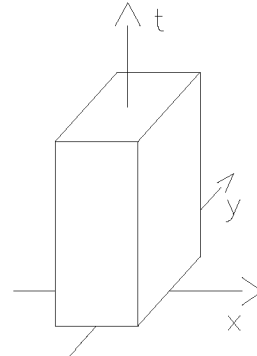


Figure 2. Projection of the Bjorken brick to  $xyt$ -space.

the Boltzmann approximation and the customary definition of the coefficient  $v_2$ , we get

$$v_2(p_t) = \frac{(t^2 - \tau_0^2) p_t K_0\left(\frac{m_t}{T}\right) (l_y - l_x)}{3 \left( \pi t m_t K_1\left(\frac{m_t}{T}\right) l_x l_y + (t^2 - \tau_0^2) p_t K_0\left(\frac{m_t}{T}\right) (l_y + l_x) \right)}. \quad (2)$$

Differential elliptic flow is now essentially controlled by three parameters: the ratio of the system size in  $x$ - and  $y$ -directions  $l_x/l_y$ , the ratio of lifetime to spatial dimension  $t/l_y$  and temperature  $T$ . The effect of thermalization time  $\tau_0$  can be compensated by changing the lifetime and therefore we prefer to keep it fixed to value  $\tau_0 = 0.6$  fm/ $c$  inspired by our hydrodynamical calculations [4].

In Fig. 3 a) the differential elliptic flow of pions obtained from this model using four different parameter sets is shown. The solid line corresponds to a case where parameter values are motivated by the values from hydrodynamical simulations of semi-central collisions ( $l_x/l_y = 0.58$ ,  $t/l_y = 1.35$ ,  $T = 140$  MeV). The qualitative behaviour of  $v_2$  is surprisingly similar to that seen in the Low Density Limit approximation [4] where the anisotropy is estimated by calculating a first order correction to the free streaming distribution. At low values of transverse momenta,  $v_2$  increases rapidly but saturates already around  $p_t = 200 - 300$  MeV/ $c$ . As demonstrated by the dashed line obtained using  $l_x/l_y = 0.5$  and  $t/l_y = 1$ , a change in the ratios scales the saturation value of  $v_2$ , but does not affect the value of  $p_t$  where saturation takes place.

The only variable which affects the slope of  $v_2(p_t)$  is the temperature of the system as shown by the dotted line ( $T = 500$  MeV). The effect is weak and even outrageous values of parameters ( $l_x/l_y = 1/15$ ,  $T=75$  GeV, dashed-dotted line) fail to reproduce the data. Therefore we may conclude that the present data cannot be described without the presence of strong transverse flow at RHIC.

The generalization of the Bjorken brick to allow transverse flow is straightforward although the resulting expression for  $v_2(p_t)$  is much more complicated than Eq. (2). In addition to the parameters mentioned earlier, we have the flow velocities in  $x$ - and  $y$ -direction  $v_x$  and  $v_y$ . This generalized parametrization allows us to check which one contributes more to the observed anisotropy: anisotropic flow field or source shape. Figure 3 b) shows our fits to the data assuming that both source shape and velocity field are anisotropic

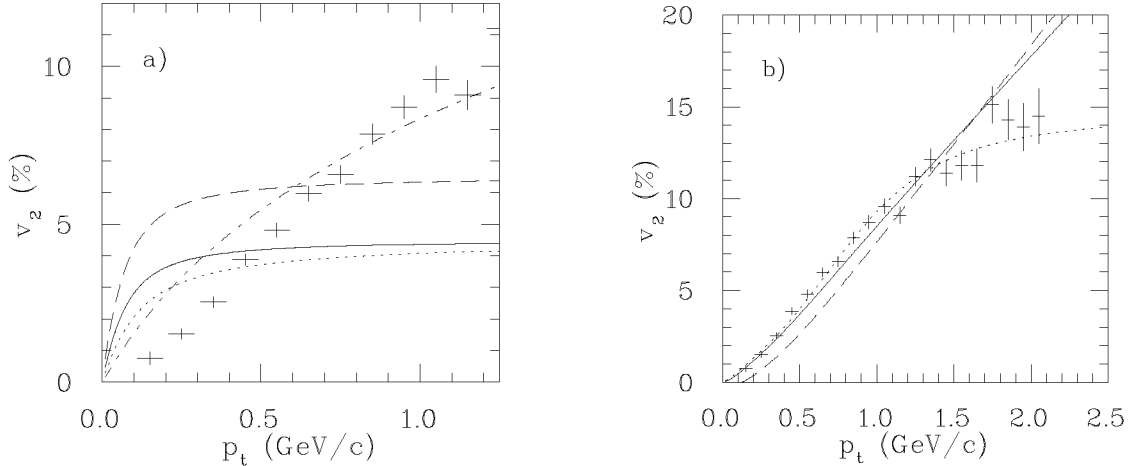


Figure 3. Differential elliptic flow of pions from Bjorken brick without flow (left) or with additional flow (right) compared to elliptic flow of charged particles at RHIC [2]. For explanation of the curves, see the text.

(solid line,  $v_x = 0.6$ ,  $v_y = 0.57$ ,  $l_x/l_y = 0.93$ ), only the velocity field is anisotropic (dashed line,  $v_x = 0.6$ ,  $v_y = 0.57$ ,  $l_x/l_y = 1$ ) or only source shape is anisotropic (dotted line,  $v_x = v_y = 0.7$ ,  $l_x/l_y = 0.73$ ). Due to the crudeness of the model the differences between these fits are not meaningful, but the data allows all three different possibilities. However, an isotropic velocity field from a deformed source depicts very interesting behaviour of saturating  $v_2$  around  $p_t = 1.5 - 2$  GeV/c, in the same region where data do. Whether this is anything but a coincidence and whether it is possible to produce this kind of behaviour using a dynamical model remains to be seen.

## 2. Hydrodynamic calculations

We have used a boost invariant hydrodynamical model [8] to describe the time evolution of the collision system at RHIC [4,5,10]. In our approach the initial conditions of the hydrodynamical evolution were fixed by scaling the initial densities used to reproduce SPS data [8] until the final particle multiplicity measured by PHOBOS collaboration [9] was reached. In the most central collisions this leads to maximum energy densities of  $\epsilon = 22.3 - 23$  GeV/fm<sup>3</sup> and temperatures of  $T = 270 - 330$  MeV, depending on the equation of state (EoS).

In Figs. 4 and 5 we show our results for minimum bias collisions obtained using two different EoS — one with a phase transition to QGP (EoS Q) and one without (EoS H). The agreement between the charged particle data and hydrodynamic calculation is excellent up to  $p_t \approx 1.5$  GeV/c where the measured elliptic flow begins to show signs of saturation to some value whereas the hydrodynamic result keeps increasing. The pion data show similar agreement independent of the EoS while at first glance the proton  $v_2(p_t)$  data seem to favour the existence of a phase transition. However, as shown in [5,10], proton elliptic flow is sensitive to freeze-out temperature and details of initial distributions, contrary to the elliptic flow of pions and charged particles. Therefore no conclusions about the EoS can be drawn without further constraints on the model. The data also show a strong

mass dependence of  $v_2(p_t)$  which is typical to hydrodynamical models: the heavier the particle, the smaller  $v_2$  at small values of  $p_t$ .

As a function of centrality (see [3,4]) our fit to data is less successful. As can be expected, we can reproduce the data in central and semi-central collisions, but we overestimate elliptic flow in peripheral collisions, due to the loss of a sufficient degree of thermalization.

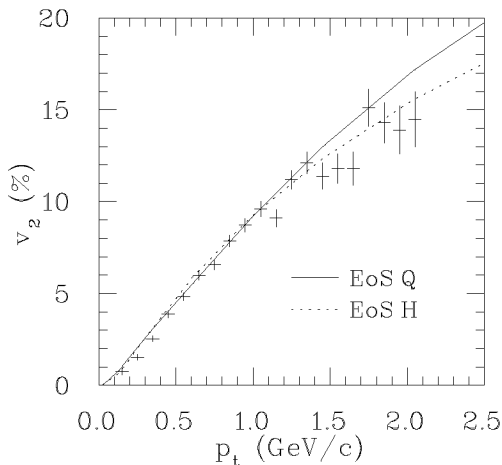


Figure 4. Differential elliptic flow of charged particles in minimum bias collisions at RHIC compared to data [2].

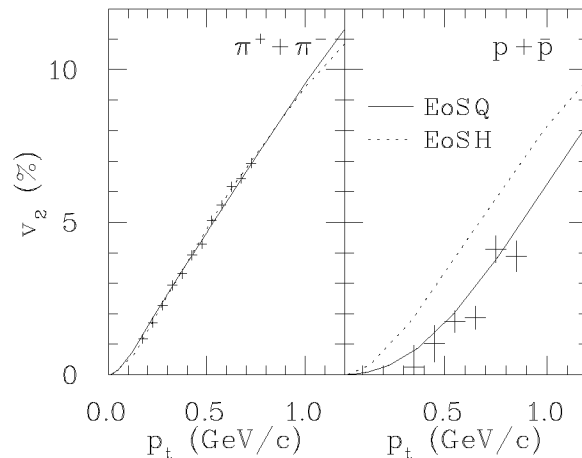


Figure 5. Differential elliptic flow of pions and protons+antiprotons in minimum bias collisions at RHIC compared to data [3].

The observed elliptic flow depends on the amount of rescatterings during the expansion. Hydrodynamics assumes zero mean free path, or equivalently, infinitely strong rescattering. It therefore provides practical upper limits for the anisotropy of particle distribution. That the experimental data reach these limiting values for elliptic flow and also reflect the mass dependence typical for a hydrodynamic system points towards early thermalization and a subsequent hydrodynamic evolution in central and semi-central collisions at RHIC.

## REFERENCES

1. J.-Y. Ollitrault, Phys. Rev. D **46** (1992) 229.
2. K.H. Ackermann *et al.* (STAR Collaboration), Phys. Rev. Lett. **86** (2001) 402.
3. R. Snellings *et al.* (STAR Collaboration), these proceedings.
4. P.F. Kolb, P. Huovinen, U. Heinz and H. Heiselberg, Phys. Lett. B **500** (2001) 232.
5. P. Huovinen *et al.* Phys. Lett. B **503** (2001) 58.
6. U.A. Wiedemann, Phys. Rev. C **57** (1998) 266.
7. K.A. Bugaev, Nucl. Phys. A **606** (1996) 559.
8. P.F. Kolb, J. Sollfrank and U. Heinz, Phys. Lett. B **455** (1999) 45; P.F. Kolb, J. Sollfrank, P.V. Ruuskanen and U. Heinz, Nucl. Phys. A **661** (1999) 349.
9. B.B. Back *et al.* (PHOBOS Collaboration), Phys. Rev. Lett. **85** (2000) 3100.
10. P.F. Kolb, U. Heinz, P. Huovinen, K.J. Eskola and K. Tuominen, hep-ph/0103234.